Virchows Archiv (1994) 425:297–304

ORIGINAL ARTICLE

Ayumi Yawata · Akio Kanzaki · Kenzo Uehira
Yoshihito Yawata

A surface replica method: a useful tool for studies of the cytoskeletal network in red cell membranes of normal subjects and patients with a β-spectrin mutant (spectrin Le Puy: $\beta^{220/214}$)

Received: 7 April 1994 / Accepted: 6 July 1994

Abstract Visualization of the components of the red cell membranes, and especially the structure of cytoskeletal proteins in situ, has become a requisite in studies of red cell membrane disorders. There has been a search for a consistent and dependable method for detecting these structures. In the present study, the surface replica method was used with transmission electron microscopy to examine the cytoskeletal network of the red cell ghosts of a normal control and patients with a β-spectrin mutant (β-spectrin Le Puy). The surface replica method is well-suited to observation of the cytoskeletal network of the membranes in a nearly native in situ condition. Immunogold labelling with anti-membrane protein antibodies is easily applicable to the identification of each component of the cytoskeletal proteins. The findings obtained under normal and pathological conditions using the surface replica method corresponded with those made by the quick-freeze, deep-etching method.

Key words Cytoskeletal network
Surface replica method · β-Spectrin Le Puy

Introduction

Great progress has been made in studies of red cell membrane disorders from the standpoint of biochemistry, biophysics and gene analysis [4, 10, 27, 28]. Visualization of these findings has become more important to verify such abnormalities [6, 7, 16, 19, 21, 22, 23, 26, 37, 38, 40, 41]. In addition, electron microscopic findings can provide precise qualitative information as well as a great deal of insight for further studies using biochemical and genetic methods. This is especially relevant to membrane research, in which the understanding of topographical structure in situ is crucial.

A. Yawata · A. Kanzaki · K. Uehira · Y. Yawata (✉)
Division of Hematology, Department of Medicine,
Kawasaki Medical School, 577 Matsushima, Kurashiki City,
Japan, 701–01

The red cell membranes are composed of a lipid bilayer and a cytoskeletal network beneath it [28]. This cytoskeletal network chiefly consists of cytoskeletal proteins; spectrins, actin, and band 4.1. The assembled cytoskeletal network is bound to integral proteins (band 3 and glycophorins) via anchor proteins (ankyrin and band 4.2). Therefore, any mutation of these membrane proteins might affect the normal structure of the membrane skeleton. The major cytoskeletal protein anomalies are spectrin mutations [4, 10, 28]. Spectrins are composed of an α-chain and a β-chain, which form spectrin dimers ($\alpha\beta$) to tetramers ($\alpha_2\beta_2$). Many mutations of α- and β-spectrins have recently been reported [4, 28], and the molecular defects in most of these mutations have been identified [10]. β-Spectrin mutations [11, 12, 13, 14, 17, 24, 30, 33, 34, 42] generally appear to be more severe clinically than α-spectrin mutations. Two mutations of β-spectrins; β-spectrin Tokyo ($\beta^{220/216}$) [17] and β-spectrin Le Puy in Yamagata [24], have been detected in the Japanese population. In these mutations, the mutated β-spectrin failed to form normal spectrin tetramers biochemically [4]. As a result, a marked impairment of the cytoskeletal network in the membrane structure due to the mutated β-spectrin is to be expected in these patients.

Several trials have been carried out to observe impaired membrane structure in hereditary elliptocytosis by electron microscopy, using a negative staining method [2, 22, 31, 36]. The findings in these studies, however, were obtained from specimens in which the cytoskeletons had been treated with detergents, such as Triton, or trypsin. Therefore, the networks were artificially over-extended and over-stretched. These specimens appear to be adequate for identifying the exact binding sites in each membrane protein, but probably be inadequate for examination of the exact membrane structure in situ in normal and abnormal conditions [3, 15, 25, 26, 35, 37, 38, 39]. Although the quick-freeze, deep-etching (QFDE) method appears to be the best method at the present time [26, 37, 38], it requires special skills and special equipment, and consistent good results are hard to obtain. In contrast, the surface replica method [32] has

been utilized widely in many fields other than the field of red cell membrane research [16, 40]. Consistent results can be obtained easily with this method, and it is easy to apply immunogold labelling with anti-membrane protein antibodies [1]. In this study, the surface replica method was utilized to observe the impaired cytoskeletal network in a nearly native in situ condition, and spectrins were identified with immunogold labelling in the red cells of a β-spectrin mutant, spectrin Le Puy ($\beta^{220/214}$).

Materials and methods

Case study. The propositus was a 60-year-old Japanese male with uncompensated haemolysis: red cell count (RBC) 2.62×10^{12}/l, haemoglobin 83 g/l, haematocrit 25.1%, mean cell haemoglobin concentration (MCHC) 33.7%, reticulocytes 12.6%, and indirect bilirubin 2.48 mg/dl. Splenectomy improved his clinical picture: RBC 4.38×10^{12}/l, reticulocytes 1.2%, and indirect bilirubin 0.4 mg/dl. Red cell morphology after splenectomy revealed elliptocytosis with some poikilocytic changes. His 36-year-old daughter had been suffering from haemolytic anaemia with elliptocytosis to the same extent prior to splenectomy, as shown in Fig. 1.

Protein chemistry revealed the presence of a mutated β-spectrin (β': apparent molecular weight 214 kDa) on sodium dodecyl sulfate polyacrylamide gel electrophoresis (SDS-PAGE) by the methods of Laemmli et al. [18] and Fairbanks et al. [8]. The content of the mutated β-spectrin (β') was 31.0% of total β-spectrins (normal β + mutated β'). Using the method of Liu et al. [20], spectrin dimer self-association was found to be impaired (Ka: 3.2×10^{5}/M; normal control 5.8±1.1 (n=75)). The content of spectrin (Sp) dimer (D) in the crude extract at 4° C was markedly increased (SpD per total spectrins: 43.2%, normal control 7.0±4.0 (n=30)). Using the method of Pothier et al. [29], the level of the αI 74 kDa fragment following limited digestion with trypsin at 22 h of incubation was increased (33.80% of total αI domain (80 kDa+74 kDa); normal control 25.12±0.42 (n=13)). These results indicate that the mutated β-spectrin (β' in this patient) failed to form tetramers with α-spectrins, leading to the impaired formation of the normal cytoskeletal network.

The mutation in the β-spectrin gene was confirmed by gene analysis with complementary and genomic DNA [24]. An A→G substitution was detected at position +4 of the 5′ donor splice site consensus sequence of intron X of the β-spectrin gene, which is exactly the same mutation reported previously as spectrin Le Puy [11]. Based on these results, it was concluded that the patient demonstrated the mutated β-spectrin (β') due to a point mutation on the β-spectrin gene, and that this led to the impaired spectrin functions. Therefore, the cytoskeletal structure was expected to be markedly impaired in this β-spectrin mutant.

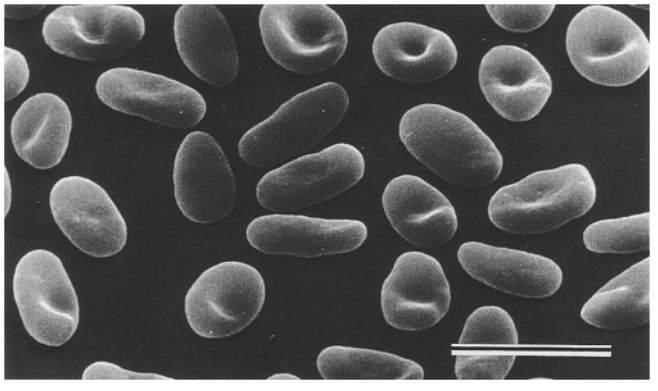

Fig. 1 Scanning electron micrograph of red cells from the peripheral blood of the daughter of the propositus with spectrin Le Puy. The presence of elliptocytosis is prominent. *Bar*=10 μm ×21,000

Red cell ghosts were prepared from freshly drawn blood at 4° C by the method of Dodge et al. [5]. The lysing buffer consisted of 5 mM sodium phosphate, 1 mM EDTA, and 0.2 mM phenylmethylsulphonyl fluoride (PMSF), pH 8.0. The red cell ghosts were thoroughly washed five times in a washing buffer (0.1 mM EDTA, 0.1 mM sodium phosphate, and 0.1 mM sodium hydroxide, pH 8.0, 1:50 v/v) to yield white ghosts.

The white ghosts were placed on a cover slip coated with 0.1% poly-L-lysine. Excessive ghosts were washed out with 5 mM phosphate buffer. After fixation with 2% glutaraldehyde solution in 0.1 M phosphate buffer at room temperature for 30 min, the ghosts were further fixed with 1% osmium tetroxide for 20 min. The fixed ghosts were subjected to dehydration with alcohol; for 5 min with 50%, 5 min with 70%, 5 min with 80%, 5 min with 90%, 10 min with 95%, 10 min twice with 99.5%, and 15 min three times with 100%, sequentially. They were then treated with isoamyl acetate for 10 min three times, and were subjected to a critical point dryer (Hitachi HCP-1, Hitachi, Tokyo, Japan). Then they were treated with platinum-paladium at an angle of 30° (1–2 nm thick) and further coated with carbon at an angle of 90° utilizing the vacuum evaporator (JEE-4X, JEOL, Tokyo, Japan). The replica (10 nm thick) was placed onto an uncoated copper grid or a grid coated with Formvar and carbon, and examined with a transmission electron microscope (JEM-2000 EXII, JEOL, Tokyo, Japan) at 120 kV.

For immunogold labelling, the washed ghosts were placed on a cover slip coated with 0.1% poly-L-lysine, and fixed with a mixture of 2% paraformaldehyde and 0.1% glutaraldehyde in an 0.1 M sodium phosphate solution for 30 min. After blocking with 1% bovine serum albumin (BSA), anti-human spectrin antibody (rabbit, polyclonal) was applied to the fixed ghosts at room temperature for 60 min in a 1 to 100 dilution with 5 mM TRIS buffer, pH 8.2 and 1% BSA. After washing with phosphate-buffered saline, gold conjugate anti-rabbit IgG (10 nm) (Biocell, Cardiff, UK) was applied at room temperature for 45 min in a 1 to 20 dilution. The ghosts were then fixed with a 2% glutaraldehyde solution, subjected to dehydration, and the replica was prepared by freezing instantaneously with liquid nitrogen with a quick freezing instrument, MF-2(Eiko, Tokyo, Japan). Deep etching and replication were performed with Balzers BAF 301 (Balzers, Lichtenstein). Etching was carried out at −100° C, 5×10^{-5} Pa for 5 min. Rotary replication was carried out with platinum at an angle of 20° (2 nm) and with carbon at an angle of 90° (10 nm). Film thickness was controlled by the frequency shift on a Balzers quartz crystal monitor (QSD 201G). The replica was placed onto copper grids (300 mesh), and subjected to transmission electron microscopy (JEM 2000-EXII, JEOL) at 200 kV.

The intact red cells were also examined for intramembrane particles (IMP) by the method of Gahmberg et al. by fixation in 1.0% glutaraldehyde, followed by impregnation with 10–40% glycerol. The red cell suspensions were rapidly frozen in liquid nitrogen, and the freeze fracture replicas were prepared in a Balzers BAF 301 apparatus (Balzers), after which they were examined with an electron microscope (JEM 2000-EXII, JEOL).

To examine the effects of heat, human mature intact red cells were treated at various temperatures; 4° C, 37° C, 40° C, 44° C, 46° C and 48° C, for 10 min each. White ghosts were prepared as described previously [40]. Thereafter, the surface replica was prepared from the white ghosts.

Results

The red cell mophology of the peripheral blood from the daughter of the propositus with the spectrin Le Puy mutation is shown in Fig. 1. A marked elliptocytosis was noted in this patient.

The white ghosts, which were fixed with 2% glutaraldehyde and then with 1% osmium tetroxide, sequentially, were subjected to critical point drying, and the replica was prepared after treatment with platinum-paladium/carbon coating. The cytoskeletal meshwork was composed of multiple smaller basic units, which were connected to each other, as shown in Fig. 2. Electron microscopy using the surface replica method revealed an orderly cobblestone-like pattern in normal subjects. The basic cytoskeletal units were reasonably extended with thinner, evenly stretched fibre filaments with well-organized junctional units. The basic cytoskeletal units can be categorized into four sizes; small (S) (12.5–25.0 nm in diameter in the shorter axis of each basic cytoskeletal unit), regular (R) (25.0–50.0 nm), medium (M) (50.0–75.0 nm), and large (L) (larger than 75.0 nm). In normal subjects, the size distributions of the units were 6±3%, 52±5%, 31±4%, and 11±3%, respectively. In making these determinations, the diameters in the shorter axis of each basic cytoskeletal unit were selected for sizing, for consistency. The diameters in the longer axis of each basic cytoskeletal unit were also measured and the results indicated essentially the same tendency as the size distributions based on the diameters in the shorter axis of each basic cytoskeletal unit, although there were slightly greater variations in the diameters in the longer axis than those in the shorter axis.

The cytoskeletal units were basically composed of thinner filaments. These filaments were 63±17 nm long and 12±4 nm wide. Knob-like structures, which were attached to the longer, thinner filaments, were also observed.

The filaments in the basic units of the cytoskeletal network were identified as spectrins by immunogold la-

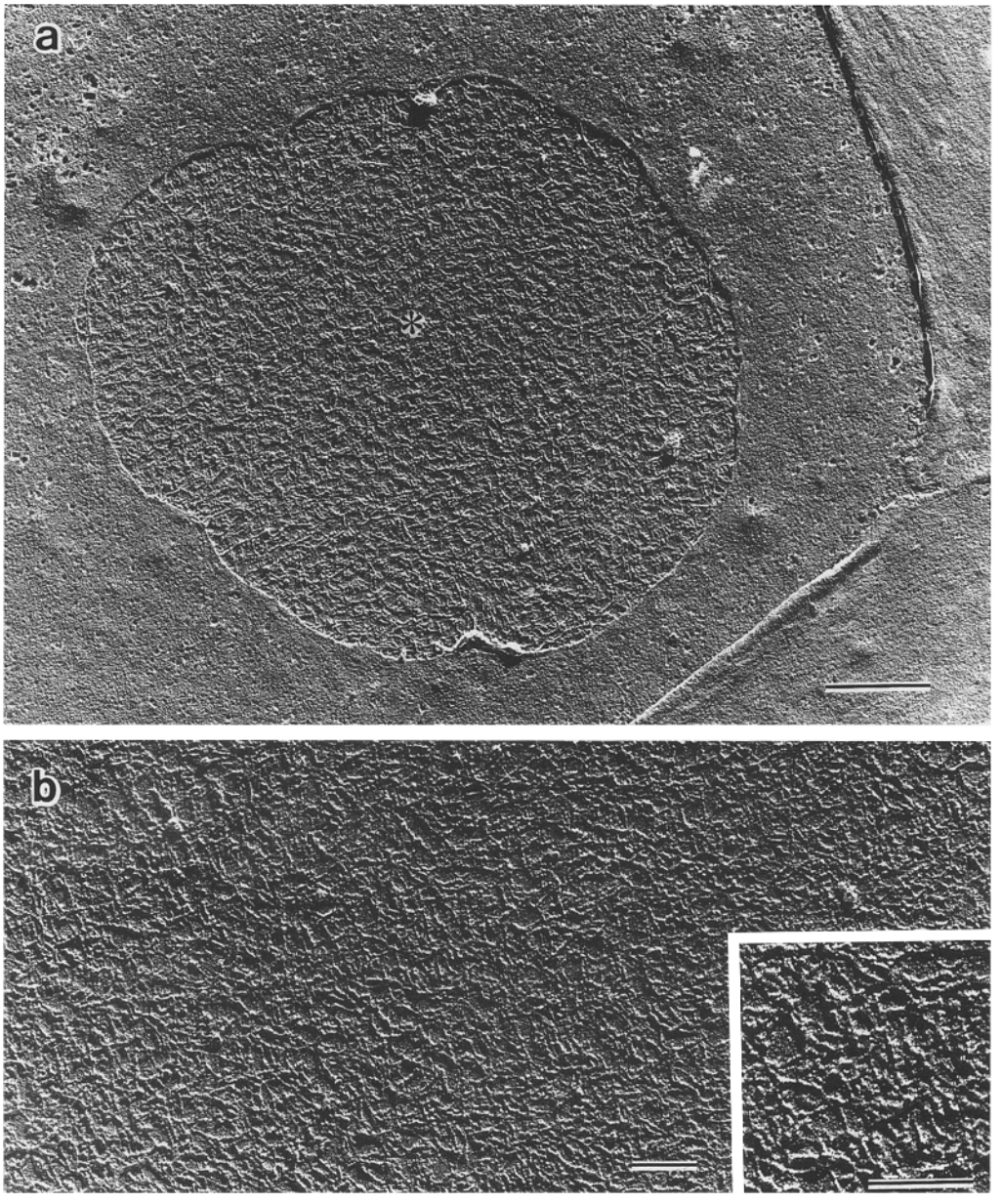

Fig. 2 Electron micrographs of the red cells of normal individuals examined by the surface replica method. **a** Lower magnification (*bar*=1 μm) ×16,000 and **b** greater magnification (*bar*=200 nm) ×47,000 with an inset (*bar*=200 nm). ×80,000. The cytoskeletal network *(asterisk)* at the centre of normal red cell ghosts as shown in **a** is visible in the single plane window. A greater magnification demonstrates an orderly cobblestone-like pattern

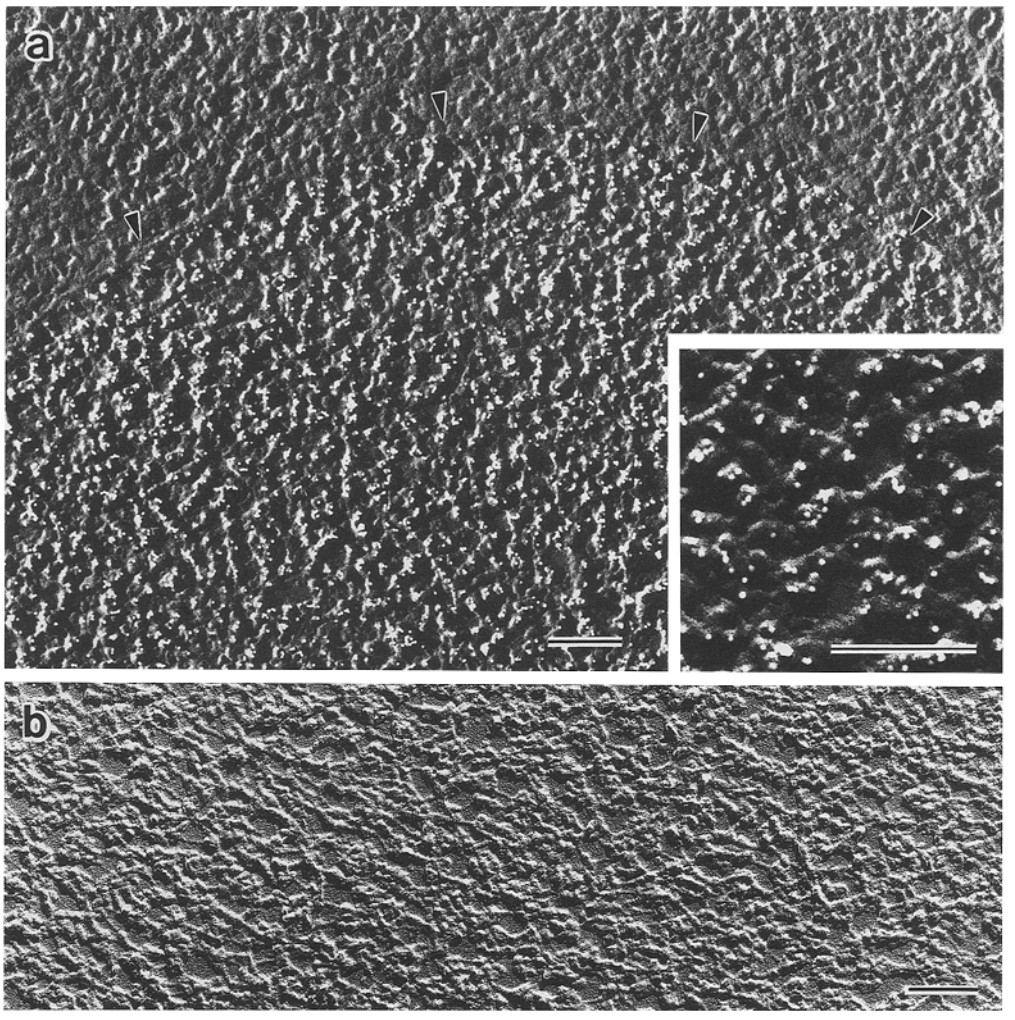

Fig. 3 Immunogold labelling of spectrin in normal red cell ghosts examined by the surface replica method. **a** A marked labelling of spectrins by immunogold particles with anti-human spectrin rabbit polyclonal antibody is seen only at the area within the single plane window, which is clearly separated from the portion of the membrane bilayer of the red cell ghosts. *Arrowheads* indicate the border of the single plane window as the membrane monolayer. **b** Control with a non-immune rabbit antibody. *Bars*=0.2 μm ×55,000 including that in inset, ×110,000

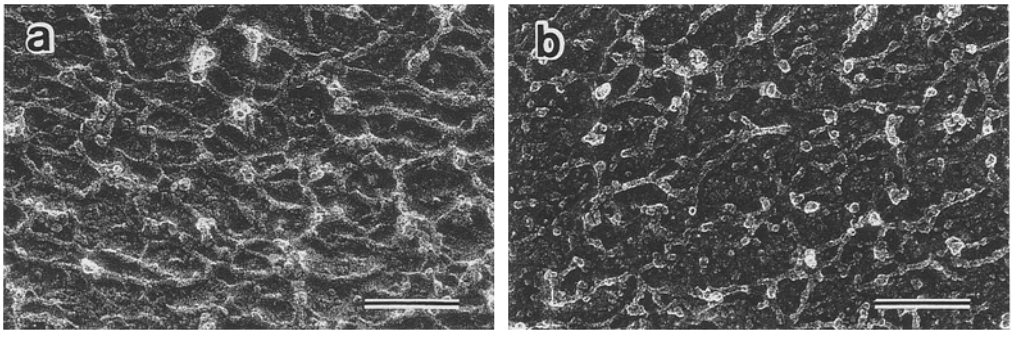

Fig. 4 Electron micrographs of the red cell cytoskeletal network examined by the quick-freeze deep-etching method. **a** A normal individual, and **b** a patient with spectrin Le Puy. A continuous orderly three-dimensional network of fine filaments and small globules is observed in a normal subject (left: **a**). ×80,000. In contrast, the structure of the cytoskeletal network in a patient with spectrin Le Puy appears disrupted with filaments of uneven lengths and widths and a reduction of the number of intersections (right: Fig. 4b). ×80,000 *Bars*=100 nm

belling with anti-human spectrin rabbit polyclonal antibody by the electron microscope (EM) with the surface replica method, as shown in Fig. 3a. The antibody recognized the fibrous components, which were present on the EM with the surface replica method, as spectrins.

It is of utmost importance to ensure the specificity of the immunolabelling. Therefore, several experiments were performed using a non-immune rabbit antibody instead of the specific anti-spectrin antibody as negative controls. The results indicated clearly that no immunogold particles were detected in these negative controls, as shown by a representative illustration in Fig. 3b.

Normal white ghosts were subjected to quick-freezing, and then to deep-etching. The replicas were prepared with platinum/carbon coating. This procedure showed that the filaments of the intact cytoskeleton existed in multi-stereotactic dimensions rather than in a single plane as shown in Fig. 4a. The filaments coated

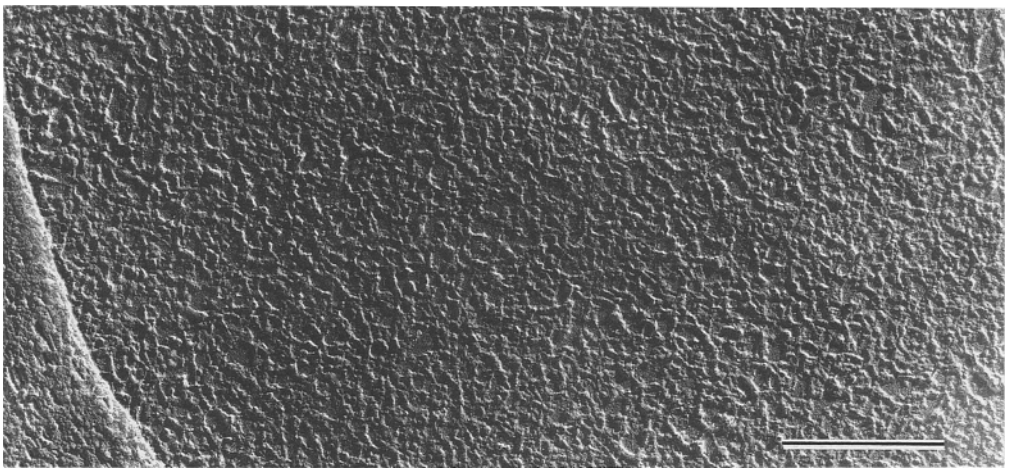

Fig. 5 Electron micrography of the red cell cytoskeletal network in red cell ghosts of spectrin Le Puy as examined by the surface replica method. The structure of the cytoskeletal network appears to be disrupted with loss of the connections among filaments, which demonstrate uneven lengths and widths and a reduction in the number of intersections. *Bar*=500 nm, ×47,000

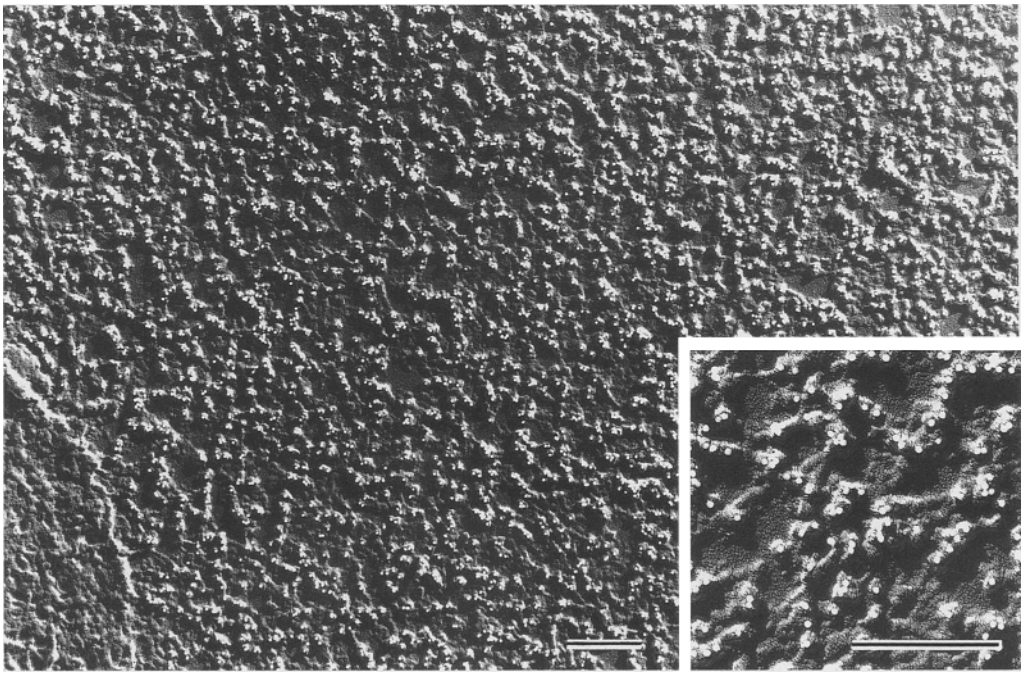

Fig. 6 Immunogold labelling of spectrins in red cell ghosts from spectrin Le Puy. Electron microscopy was performed using the surface replica method with immunogold labelling by anti-human spectrin rabbit polyclonal antibody. *Bar*=200 nm ×55,000 including that in inset, ×11,000

with platinum were 48±9 nm in length and 7±1 nm in diameter, although they appeared to be in a folded conformation, as previously reported by Ursitti et al. [38]. A total view of the cytoskeletal network showed it to be composed of numerous smaller basic units, the size of which, on the average, was 54±14 nm at the longer axis, and 23±5 nm at the shorter axis.

The membrane skeletons in spectrin Le Puy were examined by EM with the surface replica method. The results are shown in Fig. 5. The basic cytoskeletal units varied in size, and were mostly enlarged. All of the fibrous filaments appeared to lose their inter-connection with other filaments. It is interesting to note that some of the fibrous filaments had a drum-stick appearance, which probably reflected the irregularly coiled condition of these filaments. The structure of the whole red cell membranes in this disorder was clearly disorganized. Each fibrous filament was identified as spectrins by the immunogold method as shown in Fig. 6.

In spectrin Le Puy, the continuous three-dimensional network of fine filaments and small globules which had been observed in the normal control was totally disrupted with filaments of uneven lengths and width. A reduction in the number of intersections was observed by the EM with the QFDE method, as shown in Fig. 4b. The alignment of the network appeared disorderly. These findings were essentially the same as those by EM with the surface replica method. It seems difficult for abnormal β-spectrin to maintain a normal tight cytoskeletal network. As a result, the units may easily become uncoiled.

The intramembrane particles (IMP) in intact red cells were examined by the freeze fracture method using electron microscopy. The results are shown in Fig. 7. The

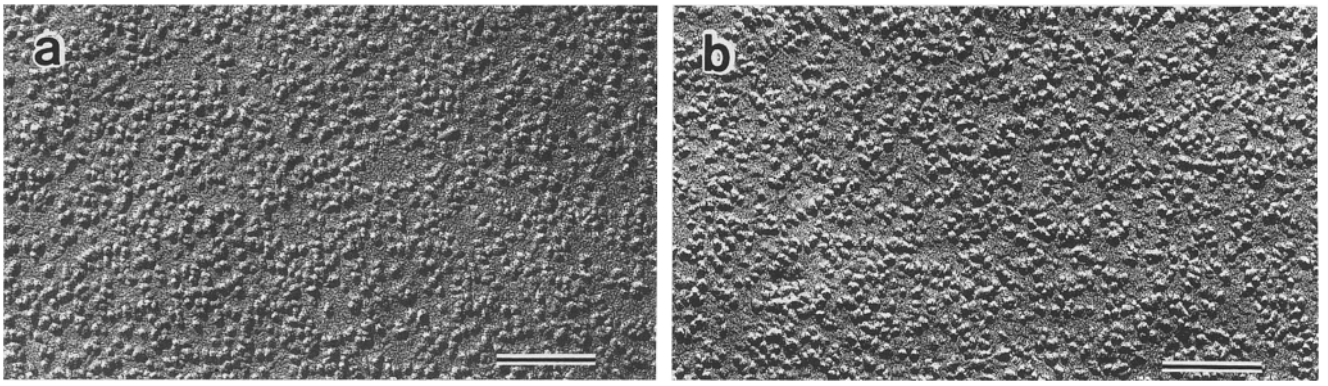

Fig. 7 Freeze-fracture images of intact red cells of a normal subject and a patient with spectrin Le Puy. Electron microscopy was performed by the freeze-fracture method in intact red cells of the normal individual (left: **a**) ×130,000 and those of the patient with spectrin Le Puy (right: **b**). ×130,000 The numbers, sizes, and distribution patterns of the intramembrane particles (IMP) were perfectly intact in the normal subject. In contrast, in spectrin Le Puy, the IMP tended to demonstrate slight clustering and uneven sizing (probably due to increased oligomerization). *Bars*=100 nm

numbers, sizes, and distributions patterns of the IMP in normal controls were perfectly intact, as shown in Fig. 7a. However, in the patient with spectrin Le Puy (Fig. 7b), the IMP tended to demonstrate slight clustering in some areas and uneven sizing (probably representing increased oligomerization of the IMP) among them. These findings may indicate that the IMP was moderately affected by the impaired cytoskeletal network caused by the gene mutation of β-spectrin.

The normal cytoskeletal network (Fig. 2) in unheated normal red cells gradually became disrupted by heating up to 48° C, at which temperature the fibrous structure appeared disconnected with the appearance of bulky aggregates (data not shown). Under the same condition at 48° C, results with the QFDE method were essentially the same as those obtained by the surface replica method.

Discussion

There has been recent progress in the field of red cell membrane disorders [27, 28] using molecular biological techniques especially with regard to spectrin anomalies [4, 10]. Compared with numerous reported cases of α-spectrin mutations, β-spectrin anomalies are relatively rare, and only nine variants have been reported [11, 12, 13, 14, 17, 24, 30, 33, 34, 42], two of which were identified at Kawasaki Medical School [17, 24]. On these mutations of β-spectrin in human red cells, it was determined that there were varying degrees of truncation of the C-terminal region of β-spectrin based on molecular abnormalities [4]. In contrast to spectrin Rouen ($\beta^{220/218}$) [13] with the least truncation, spectrin Le Puy ($\beta^{220/218}$) [11] demonstrated the most marked truncation of β-spectrin. Spectrin Tokyo ($\beta^{220/216}$) [17], Spectrin Nice ($\beta^{220/216}$) [34], Spectrin Tandil [14], Spectrin Göttingen ($\beta^{220/216}$) [42], Spectrin Cagliari [30] and Spectrin Providence [12] are in between. It is known that the C-terminal region of β-spectrin is bound to the N-terminal region of α-spectrin ($\alpha^{I/80}$). The head-to-head contact of α- and β-spectrins initiates the formation of hetero-tetramer ($\alpha_2\beta_2$). Therefore, truncation at the C-terminal region of β-spectrin is expected to induce impairment of the head-to-head association between α- and β-spectrins. Morphologically, the impairment of the association should be indicative of disruption of the cytoskeletal network; that is, a disconnection of the fibrous filaments with uneven lengths and widths, and a reduction in the number of intersections. Among the various β-spectrin mutants described above, the red cell membrane skeletal network would be most impaired in Spectrin Le Puy [11, 24], because the mutation of the β-spectrin gene in Spectrin Le Puy is known to deduce maximal truncation of the C-terminal region of β-spectrin. Therefore, we selected spectrin Le Puy for this study.

Initially, visualization of the cytoskeletal network was carried out by the negative staining method with electron microscopy [2, 22, 31]. That method demonstrates a two-dimensional network of chiefly hexagonal structure composed of approximately 200 nm long spectrin tetramers. However, the negative staining method is linked to a procedure by which the red cell membrane ghosts are treated with chemical reagents to make the membrane skeleton spread. Therefore, several attempts have been made to visualize the red cell membrane cytoskeleton in situ under its native condition [3, 15, 25, 26, 35, 37, 38, 39, 40] rather than under an artificially stretched condition. The replica method with the QFDE technique for electron microscopy appears to provide the best resolution for visualization of the in situ condition of the cytoskeletal network [26, 37, 38, 40]. This method clearly discloses the filamentous network of the intact cytoskeleton.

With the QFDE technique for electron microscopy, however, it is quite difficult to obtain an adequate surface of the cytoskeletal network consistently under regular experimental conditions. Furthermore, it requires special equipment, such as the Balzers BAF-301 (Balzers). With the surface replica method, however, such special equipment is unnecessary, and reliable results nearly equal to those achieved with the QFDE method can be obtained.

In addition, the surface replica method is even more useful than the QFDE method, since the immunogold method is easily applicable with the surface replica method for identification of the specific components of the cytoskeletal network with specific antibodies. By the QFDE method, specimens of red cell membrane ghosts should be frozen instantaneously to −196° C. As a result, immunocytochemistry is absolutely impossible. By the surface replica method, however, immunocytochemistry is feasible, because the red cell membrane ghosts are treated at 4° C thoughout the procedure.

Our findings using the surface replica method appear to demonstrate an impaired cytoskeletal network in the red cells of the β-spectrin mutant (spectrin Le Puy) almost as reasonally and adequately as those obtained by the QFDE method, as shown by our previous study [24].

Experimentally, the red cell membranes were manipulated by heat treatment to induce impairment of the cytoskeletal network. With the surface replica method, it was possible to detect abnormalities in the cytoskeletal network sequentially under various temperatures. The abnormalities in spectrin as a component of the cytoskeletal network were also identified by the immunogold method with rabbit anti-human spectrin polyclonal antibodies.

In summary, the surface replica method appears to be useful for the detection of abnormalities in the cytoskeletal network in a nearly native in situ condition.

Acknowledgements The authors wish to thank Dr. Kaoru Takanashi of Honma Hospital, Sakai City, Japan and Professor Akira Miura of the Third Department of Internal Medicine, Akita University School of Medicine for kindly supplying us with the blood specimens. They also would like to thank Professor Jean Delaunay and his colleagues for their critical discussion and advice. This study was supported in part by a research grant for Idiopathic Disorders of Hematopoietic Organs from the Japanese Ministry of Health and Welfare, by Grants-in-Aid for Scientific Research (No. 04671540, 05670936 and 06671120) and International Scientific Research Program: Joint Research (No. 06044212) from the Ministry of Education, Science and Culture of the Japanese Government, by the Japan Society for the Promotion of Science (JSPS)-the Centre National de la Recherche Scientifique (CNRS) Joint Research Projects, and by research grants from Kawasaki Medical School (No. 4–301, 5–101and 6–106).

References

1. Bohn W, Röser K, Hohenberg H, Mannweiler K, Traub P (1993) Cytoskeleton architecture of C6 rat glioma cell subclones differing in intermediate filament protein expression. J Struct Biol 111:48–58
2. Byers TJ, Branton D (1985) Visualization of the protein associations in the erythrocyte membrane skeleton. Proc Natl Acad Sci USA 82:6153–6157
3. Coleman TR, Fishkind DJ, Mooseker MS, Morrow JS, (1989) Functional diversity among spectrin isoforms. Cell Motil Cytoskeleton 12:225–247
4. Delaunay J, Dhermy D (1993) Mutations involving the spectrin heterodimer contact site: clinical expression and alterations in specific function. Semin Hematol 30:21–33
5. Dodge JT, Mitchell C, Hanahan DJ (1963) The preparation and chemical characteristics of hemoglobin-free ghosts of human erythrocytes. Arch Biochem Biophys 100:119–130
6. Elgsaeter A, Branton D (1974) Intramembrane particle aggregation in erythrocyte ghosts. I. The effect of protein removal. J Cell Biol 63:1018–1030
7. Elgsaeter A, Shotton DM, Branton D (1976) Intramembrane particle aggregation in erythrocyte ghosts. II. The influence of spectrin aggregation. Biochim Biophys Acta 426:101–122
8. Fairbanks G, Steck TL, Wallach DFH (1971) Electrophoretic analysis of the major polypeptides of the human erythrocyte membrane. Biochemistry 10:2606–2617
9. Gahmberg CG, Taurén G, Virtanen I, Wartiovaara J (1978) Distribution of glycophorin on the surface of human erythrocyte membranes and its association with intramembrane particles: an immunochemical and freeze-fracture study of normal and En(a-) erythrocytes. J Supramol Struct 8:337–347
10. Gallagher PG, Forget BG (1993) Spectrin genes in health and disease. Semin Hematol 30:4–20
11. Gallagher PG, Tse WT, Costa F, Scarpa A, Boivin P, Delaunay J, Forget BG (1991) A splice site mutation of the β-spectrin gene causing exon skipping in hereditary elliptocytosis associated with a truncated β-spectrin chain. J Biol Chem 266:15154–15159
12. Gallagher PG, Tse WT, Mohandas N, Marchesi SL, Forget BG (1992) Spectrin Providence: a defect of erythrocyte beta spectrin ($\beta^{2019\ Ser\rightarrow Pro}$) homozygosity for which is associated with fatal hydrops fetalis. Blood 80 [Suppl 1]:145a
13. Garbarz M, Tse WT, Gallagher PG, Picat C, Lecomte MC, Galibert F, Dhermy D, Forget BG (1991) Spectrin Rouen ($\beta^{220-218}$), a novel shortened β-chain variant in a kindred with hereditary elliptocytosis. Characterization of the molecular defect as exon skipping due to a splice site mutation. J Clin Invest 88:76–81
14. Garbarz M, Boulanger L, Pedroni S, Lecomte MC, Gautero H, Galand C, Boivin P, Feldman L, Dhermy D (1992) Spectrin β^{Tandil}, a novel shortened β-chain variant associated with hereditary elliptocytosis is due to a deletional frameshift mutation in the β-spectrin gene. Blood 80:1066–1073
15. Heuser J (1989) Protocol for 3-D visualization of molecules on mica via the quick-freeze, deep-etch technique. J Electron Microsc Tech 13:244–263
16. Inoue T, Kanzaki A, Yawata A, Tsuji A, Ata K, Okamoto N, Wada H, Higo I, Sugihara T, Yamada O, Yawata Y (1994) Electron microscopic and physicobiochemical studies on disorganization of the cytoskeletal network and integral protein (band 3) in red cells of band 4.2 deficiency with a mutation (codon 142: GCT→ACT). Int J Hematol 59:157–175
17. Kanzaki A, Rabodonirina M, Yawata Y, Wilmotte R, Wada H, Ata K, Yamada O, Akatsuka J, Iyori H, Horiguchi M, Nakamura H, Mishima T, Morlé L, Delaunay J. (1992) A deletional frameshift mutation of the β-spectrin gene associated with elliptocytosis in spectrin Tokyo ($\beta^{220/216}$). Blood 80:2115–2121
18. Laemmli UK (1970) Cleavage of structural proteins during the assembly of the head of bacteriophage T4. Nature 227: 680–685
19. Liu S-C, Derick LH (1992) Molecular anatomy of the red blood cell membrane skeleton: structure-function relationships. Semin Hematol 29:231–243
20. Liu S-C, Palek J, Prchal J, Castleberry RP (1981) Altered spectrin dimer-dimer association and instability of erythrocyte membrane skeletons in hereditary pyropoikilocytosis. J Clin Invest 68:597–605
21. Liu S-C, Windisch P, Kim S, Palek J (1984) Oligomeric states of spectrin in normal erythrocyte membranes: biochemical and electron microscopic studies. Cell 37:587–594
22. Liu S-C, Derick LH, Palek J (1987) Visualization of the hexagonal lattice in the erythrocyte membrane skeleton. J Cell Biol 104:527–536
23. Liu S-C, Derick LH, Agre P, Palek J (1990) Alteration of the erythrocyte membrane skeletal ultrastructure in hereditary spherocytosis, hereditary elliptocytosis and pyropoikilocytosis. Blood 76:198–205
24. Maréchal J, Wada H, Koffa T, Kanzaki A, Wilmotte R, Ikoma K, Yawata A, Inoue T, Takanashi K, Miura A, Alloisio N, Del-

aunay J, Yawata, Y (1994) Hereditary elliptocytosis associated with spectrin Le Puy in a Japanese family. Ultrastructural aspect of the red cell skeleton. Eur J Haematol 52:92–98
25. Nermut MV (1981) Visualization of the "membrane skeleton" in human erythrocytes by freeze-etching. Eur J Cell Biol 25: 265–271
26. Ohno S, Terada N, Fujii Y, Ueda H, Kuramoto H, Kamisawa N (1993) Immunocytochemical study of membrane skeletons in abnormally shaped erythrocytes as revealed by a quick-freezing and deep-etching method. Virchows Arch [A] 422:73–80
27. Palek J, Sahr KE (1992) Mutation of the red blood cell membrane proteins: from clinical evaluation to detection of the underlying genetic defect. Blood 80:308–330
28. Palek J, Jarolim P (1993) Clinical expression and laboratory detection of red blood cell membrane protein mutations. Semin Hematol 30:249–283
29. Pothier B, Alloisio N, Maréchal J, Morlé L, Ducluzeau MT, Caldani C, Philipe N, Delaunay J (1990) Assignment of Sp$\alpha^{I/74}$ hereditary elliptocytosis to the α- and β-chain of spectrin through in vitro dimer reconstitution. Blood 75:2061–2069
30. Sahr KE, Coetzer TL, Moy LS, Derick LH, Chishti AH, Jarolim P, Lorenzo F, Miraglia Del Giudice E, Iolascon A, Galanello R, Cao A, Delaunay J, Liu S-C, Palek J (1993) Spectrin Cagliari: an Ala to Gly substitution in helix 1 of β spectrin repeat 17 that severely disrupts the structure and self-association of the erythrocyte spectrin heterodimer. J Biol Chem 268: 22656–22662
31. Shen BW, Josephs R, Steck TL (1986) Ultrastructure of the intra-skeleton of the erythrocyte membrane. J Cell Biol 102: 997–1006
32. Smith SB, Revel JP (1972) Mapping of concanavalin A binding sites on the surface of several cell types. Dev Biol 27: 434–441
33. Tse WT, Lecomte MC, Costa FF, Garbarz M, Féo C, Boivin P, Dhermy D, Forget BG (1990) Point mutation in the β-spectrin associated with $\alpha^{I/74}$ hereditary elliptocytosis. J Clin Invest 86:909–916
34. Tse WT, Gallagher PG, Pothier B, Costa FF, Scarpa A, Delaunay J, Forget BG (1991) An insertional frameshift mutation of the β-spectrin gene associated with elliptocytosis in spectrin Nice ($\beta^{220/216}$). Blood 78:517–523
35. Tsukita S, Tsukita S, Ishikawa H (1980) Cytoskeletal network underlying the human erythrocyte membrane. J Cell Biol 85:567–576
36. Tyler JM, Hargreaves WR, Branton D (1979) Purification of two spectrin-binding proteins: biochemical and electron microscopic evidence for site-specific reassociation between spectrin and bands 2.1 and 4.1 Proc Natl Acad Sci USA 76:5192–5196
37. Ursitti JA, Wade JB (1993) Ultrastructure and immunocytochemistry of the isolated human erythrocyte membrane skeleton. Cell Motil Cytoskeleton 25:30–42
38. Ursitti JA, Pumplin DW, Wade JB, Bloch RJ (1991) Ultrastructure of the human erythrocyte cytoskeleton and its attachment to the membrane. Cell Motil Cytoskeleton 19:227–243
39. Weinstein RS, Tazelaar HD, Loew JM (1986) Ultrastructure of axial elongation of the membrane skeleton. Blood Cells 11:343–357
40. Yawata Y (1994) Red cell membrane protein band 4.2: phenotypic, genetic and electron microscopic aspects. Biochim Biophys Acta 1204:131–148
41. Yawata Y (1994) Band 4.2 abnormalities in human red cells. Am J Med Sci 307:190–203
42. Yoon SH, Yu H, Eber S, Prchal JT (1991) Molecular defect of truncated β-spectrin associated with hereditary elliptocytosis. β-Spectrin Göttingen. J Biol Chem 266:8490–8494